Current noise in barrier photoconducting devices. I. Theory

A. Carbone and P. Mazzetti
Dipartimento di Fisica del Politecnico di Torino, Corso Duca degli Abruzzi 24, 10129 Torino, Italy
(Received 16 August 1993)

A theory of current noise in photoconducting devices, developed on the basis of a large set of measurements concerning the behavior of photoconductivity, photoresponsivity, and noise as a function of light intensity and wavelength in CdS-based photoconductors, is presented. The theory is based on a barrier-type photoconduction model and embodies, in a single general expression of the noise power spectrum, the contributions due to the generation recombination and to the flicker noise (*intrinsic noise*) as well as to the noise generated by the fluctuation of the potential barrier that controls the electron injection from the metal electrode into the conduction band of the photoconducting material (*photoinduced noise*). According to the model, the height of this barrier depends on a balance effect between the light-induced positive static charge (ionized deep donor centers or trapped holes) and the negative space charge due to the injected electrons. The fluctuation of the number of ionized centers or trapped holes causes a fluctuation of the potential barrier and thus of the conductance of the device. The transport process is described as a stream of conduction electrons crossing the fluctuating potential barrier and undergoing thermally activated trapping-detrapping processes within the photoconductor bulk. General expressions for the behavior of the photoconductance vs light intensity and for the photoconductance fluctuation power spectrum are worked out on the basis of this model and checked in the following paper by comparison with the experimental results. As shown there, the theory accounts for the shape and the relative changes of the noise power spectra, when the light intensity and the wavelength are varied, without any free parameter. The absolute value of the noise power density is also well reproduced without free parameters in the low-frequency range, where the photoinduced noise dominates. At higher frequencies, where the intrinsic noise becomes important, the noise power spectrum is also nicely fitted with very reasonable values of those quantities that have not been directly measured on the device. The same values of the quantities giving the correct photoconductance fluctuation spectra also reproduce the photoconductance vs light intensity curve calculated according to the proposed barrier photoconductance model.

I. INTRODUCTION

Current noise measurements in photoconducting devices can be used to obtain important information on the physical mechanisms ruling the conduction process. By comparing experimental power spectra, obtained under different physical conditions, with the results of a theory developed on the basis of a suitable photoconduction model, a check of the model itself can be performed.

An extensive theoretical investigation concerning different sources of noise in a photoconductor has been made by Van Vliet and Blok.[1–4] The analysis concerns the effect of the spontaneous fluctuations of the photon flux, taking into account Bose-Einstein statistics, generation-recombination noise produced by transitions between two or more levels, thermal and shot noise related to diffusion and injection-extraction of electrons at the electrodes. An experimental check of the noise theory developed in papers 1 and 2 is reported in Ref. 5. Electron mobility modulation due to the fluctuation of intergrain barriers in the ambit of the barrier photoconductivity theories has been considered by Petritz and Lummis.[6,7]

Other authors[8–14] have considered particular aspects of the photoconduction noise. The interpretation was generally based on the Van Vliet theory, but specific assumptions, concerning the $1/f$ noise component generated by trapping levels localized near the electrodes and the electron mobility fluctuations due to inhomogeneities within the photoconducting material were also introduced.

More recent papers in this field are mainly devoted to practical aspects related to the performance of the photoconducting device or, on the contrary, to theoretical analysis of the fluctuations in presence of light.[15–18] In these papers specific aspects of the noise power spectrum have been accounted for, but a number of free parameters have always been introduced to obtain a suitable agreement with the experimental results. The lack of a paper reporting a complete set of measurements, optical and electrical, made on the same specimen on which noise measurements are performed and extended over a wide range of light intensities and wavelengths, prevents the possibility of a complete check of any theory of current noise based on a particular photoconduction model.

In the present paper we report on a theory of current noise based on a barrier-type photoconduction model. In addition to an important aspect concerning the effect of the barrier fluctuation, this theory embodies most of the results of the previous theories (generation-recombination, $1/f$, and shot noise) in a single compact expression of the noise power spectrum. All the parameters entering this expression have a clear physical meaning and can be obtained by suitable measurements per-

0163-1829/94/49(11)/7592(11)/$06.00

formed on the same specimen. This allowed us to check many aspects of the theory without introducing any free parameter.

As shown in the following paper (hereafter referred to as paper II), the theory permits us to explain the shape and the magnitude of the power spectrum as well as its variations with the wavelength and intensity of light. In particular the theory accounts for the strong variation of the amplitude and slope of the power spectrum occurring when the light wavelength is varied in correspondence with the critical value λ_{gap}, the device conductance being kept constant by varying the light intensity.

The relative variations of the noise power density when the light intensity is varied in a range covering about three orders of magnitude are reproduced without free parameters. The observed change from a near-Lorentzian to a $1/f$-shaped power spectrum, when the light intensity is decreased below a given threshold, is explained by the theory as due to the gradual decrease of the noise component related to the barrier fluctuation.

A further confirmation of the theory is reported in a recent paper[19] concerning the effect of temperature on the photocurrent noise. The strong changes that temperature variation produces on several quantities appearing in the theoretical expression of the power spectrum of the photocurrent noise were shown to be consistent with the changes actually observed experimentally.

The theory has been tested against an extensive set of experimental results (reported in paper II) concerning photoconductance, photoresponsivity, photocurrent decay, and noise power spectra taken at different light intensities and wavelengths on the same CdS-based photoconducting device having a very low dark conductance value (lower than 10^{-9} S).

The behavior of the noise spectra versus light wavelength has also been tested on CdSe-based photoconductors and, except for the different value of the critical wavelength (500 nm for CdS and 720 nm for CdSe), very similar results have been obtained.[20]

II. PHOTOCONDUCTION MODEL

Before developing a theory of current noise in photoconductors, some basic aspects of the photoconduction mechanism must be introduced. In the present paper the main assumption concerning this mechanism is related to the so-called *theory of barrier photoconductivity,*[21] whose main aspects are briefly described below.

Barriers to free charge carriers in a metal-photoconductor-metal device may be present either at the metal-photoconductor interface or at grain boundaries in polycrystalline materials.[22]

Different mechanisms are introduced to explain the dependence of these barriers on the light intensity. In the case of polycrystalline materials, it is assumed that the barrier is lowered by the trapping of either holes or electrons in deep traps or in localized states at the grain interface.[6,23,41] For what concerns the electrode-photoconductor interface, models have been developed for the rectifying as well as for the ohmic contacts.[22,24,25]

Even if the photoconduction noise theory developed in the following can be easily extended to the case of a distributed set of light sensitive barriers, the experimental results reported in paper II are consistent with the assumption that the excess noise related to the presence of the barrier is due to the fluctuation of the height of a single barrier localized near the metal-photoconductor interface. Actually, the absolute noise intensity due to the *normal* fluctuations of the trapped charge turns out to be in good agreement with a single barrier model. Multiple barriers at grain boundaries would smooth out the fluctuation, leading to a much lower photoinduced current noise than the one observed.

As stated in the Introduction, we consider a photoconducting device consisting of a thin film of photoconducting insulator with symmetric ohmic contacts (e.g., CdS with indium electrodes[26]). Also in the case of matching work functions between metal and photoconductor and in the absence of surface states, a potential barrier can be present near the metal electrodes, depending on the difference between the work function ϕ_s and the electron affinity χ_s of the material.[27] Such a difference, which in a near intrinsic semiconductor corresponds roughly to half band gap, is sufficiently large in insulating photoconductors to prevent electrical conduction in the dark even if the contact is ohmic.

In the presence of light of suitable wavelength, ionization of deep donor centers or creation of electron-hole pairs occurs. If trapping of holes or ionization of deep donor centers is allowed, a positive space charge builds up, which lowers the metal-photoconductor barrier height, thus determining the photoconducting behavior of these devices. This is the case of CdS and of other insulating photoconductors.

In Appendix B the photoconduction model sketched above is quantitatively developed. Such a development is not strictly necessary to work out the theory of current noise, since a linearization of the dependence of the photoconductance on the positive trapped charge under light biasing conditions is allowed by the smallness of the fluctuation and, on the other hand, the parameters entering the final expression of the noise power spectrum can directly be measured on the device. However, it is reported here because the fact that the model accounts for the behavior of both the photoconductance and the photoconductance noise power spectrum of the device in an extended range of light intensities and wavelengths is a further confirmation of the model itself.

Let us now consider how the different processes are related to the photocurrent noise. Several sources of noise can be envisaged in the photoconduction model sketched above. Apart from thermal noise, which will not be considered further in the following, three sources of current noise will be taken into account in the theory developed in the following section.

A first noise source is related to the fluctuation of the barrier height, due to the fluctuation of the number of ionized donor centers or trapped holes in steady state conditions. Since the lifetime of the positive trapped charge depends on light wavelength and intensity, the power spectrum of the current noise related to the barrier height fluctuation will also be dependent on these quantities. This noise source also includes the shot noise due to the electron injection from the electrode into the photoconducting material.

The other two noise sources are inherent to the conduction processes within the photoconductor bulk. Since electrons are injected in the conduction band, before recombination with ionized deep donor centers or with holes in the valence band, a quasithermal equilibrium condition exists. This is characterized by an electron quasi-Fermi level slightly below the conduction band. In these conditions, electron trapping processes in shallow centers or in surface states, balanced by thermal excitations from these states, cause generation recombination and flicker noise. These last two noise sources, normally detected in semiconductors, can be observed in photoconductors at low light intensities or in the high-frequency part of the spectrum, where the photoinduced noise related to the barrier height fluctuation becomes negligible, as shown by the theory and confirmed by the experiments reported in paper II.

III. NOISE THEORY

On the basis of the photoconduction model sketched in the preceding section and described in detail in Appendix B, the whole transport process causing the photocurrent noise will be considered as a stochastic superposition of nonindependent current pulses.[28] These pulses are related to the injection into the conduction band of the photoconductor and to the trapping-detrapping processes that each free electron undergoes during its drift toward the anode. Both the injection process and the trapping-detrapping processes are noisy.

We will call *photoinduced noise* the excess noise related to the fluctuation of the electrode-photoconductor barrier height, determined by the fluctuation of the number of ionized deep donor centers or trapped holes produced by light. The barrier height fluctuation modulates the stream of electrons injected in the conduction band of the photoconductor and thus the stream of current pulses related to them.

The current noise created by thermally activated trapping-detrapping processes involving the generation-recombination and the flicker noise sources can be envisaged as an *intrinsic noise,* because it is typical of the conduction process within any semiconducting material.

Obviously these two noise components are not simply additive, but, as will be shown in the following, the total noise power spectrum can still be written as the superposition of an intrinsic and a photoinduced noise component arising from the modulation of the injected current.

Disregarding for the time being this modulation process, the stream of current pulses causing the photocurrent can be considered, according to the classical theories of $1/f$ and generation-recombination noise in semiconductors,[29] as a superposition of independent trains of Poisson distributed rectangular pulses of individual length $\tau_g^{(i)}$, characterized by an average length $\langle \tau_g^{(i)} \rangle$ and an exponential length distribution:

$$P_1(\tau_g^{(i)}) = \frac{1}{\langle \tau_g^{(i)} \rangle} \exp(-\tau_g^{(i)} / \langle \tau_g^{(i)} \rangle) \ . \tag{3.1}$$

The set of pulse trains characterized by the same value of $\langle \tau_g^{(i)} \rangle$ is attributed to a given type of trapping or recombination center, whose number will be proportional to $1/\langle \tau_g^{(i)} \rangle$, if a flat distribution of activation energies or of tunnelling barrier widths is assumed.[29] Since, under the same hypothesis, the average number of pulses per unit time in each train is also proportional to $1/\langle \tau_g^{(i)} \rangle$, we obtain a probability distribution function $P_2(\langle \tau_g^{(i)} \rangle)$ proportional to $1/\langle \tau_g^{(i)} \rangle^2$. This distribution can also be obtained with other assumptions.[30–34] Taking into account also the existence of a *g-r* noise component, which has a Lorentzian spectrum with a cutoff frequency $f_s = 1/2\pi\tau_s$, this function can be written as

$$P_2(\langle \tau_g^{(i)} \rangle) = K_1 \frac{1}{\langle \tau_g^{(i)} \rangle^2} + K_2 \delta(\langle \tau_g^{(i)} \rangle - \tau_s)$$

$$[\tau_{g1} < (\langle \tau_g^{(i)} \rangle) < \tau_{g2}] \ , \tag{3.2}$$

Equations (3.1) and (3.2) describe a stream of pulses giving rise to a current whose fluctuation is characterized by a $1/f$ as well as by a Lorentzian spectral component corresponding to the generation-recombination noise.

In the standard theory of current noise in semiconductors, the constants K_1 and K_2, determining the relative amplitude of these components, are calculated on the basis of specific models concerning the processes of generation recombination and trapping-detrapping of the carriers. The quantities τ_{g1} and τ_{g2} are, respectively, the lower and upper limit of $\langle \tau_g^{(i)} \rangle$. It is useful to introduce another quantity τ_g, which is the average value of $\langle \tau_g^{(i)} \rangle$ according to $P_2(\langle \tau_g^{(i)} \rangle)$,

$$\tau_g = \int_{\tau_{g1}}^{\tau_{g2}} \langle \tau_g^{(i)} \rangle P_2(\langle \tau_g^{(i)} \rangle) d(\langle \tau_g^{(i)} \rangle) \ . \tag{3.3}$$

The explicit expression of τ_g is worked out in Appendix A.

Now we will take into account that the stream of current pulses described above is further modulated by the fluctuation of the potential barrier that controls the electron injection. From the statistical point of view, the noise can still be considered to be generated by a superposition of rectangular pulse trains characterized by a wide distribution of pulse lengths, given by Eqs. (3.1) and (3.2). Each train is generated by the processes of ionization and neutralization of a single deep donor center (or by the creation and annihilation of a trapped hole), which enhances or reduces the probability of electron injection.

Since the ionization processes relative to different donor centers are assumed to be independent and the photocurrent fluctuation is small, the total noise power spectrum is given by the sum of the spectra of the elementary pulse trains produced by the ionization neutralization of each single center, the number of all the other ionized centers being kept constant and equal to its average value. Obviously it would be wrong to assume that the photocurrent is the sum of the set of pulse trains generated in this way by each center: the model is correct only to evaluate the fluctuation of the photocurrent with respect to its average value.

Each train is essentially characterized by the quantities $\tau_d^{(j)}$ and $\tau_r^{(j)}$, representing the average time intervals when the center j is, respectively, ionized or neutral. The index j is used here to characterize different types of centers having different values of $\tau_d^{(j)}$ and $\tau_r^{(j)}$ under the same illumination conditions, a fact that can be attributed to their different localization both in space and in energy.

We are dealing with a sort of random telegraph process that *modulates* the elementary pulse density within the train. The power spectrum of such a pulse train cannot simply be obtained by the well-known Machlup expression.[43] The pulses occurring in each train are characterized by a length distribution given by $P_1(\tau_g^{(i)})$ and $P_2(\langle \tau_g^{(i)} \rangle)$, as described above, and are spaced in time according to a distribution function $Q(x)$ which represents the probability density of the time interval x separating subsequent pulses within the train. A suitable distribution function $Q(x)$, which describes the situation discussed above, is given below. The elementary pulses within each train are clustered in the time interval Δt_d and are absent in the contiguous time interval Δt_r. As in a random telegraph signal, these intervals are distributed according to the two Poisson exponentials

$$P_d(\Delta t_d) = \frac{1}{\tau_d^{(j)}} \exp\left[\frac{-\Delta t_d}{\tau_d^{(j)}}\right], \tag{3.4}$$

$$P_r(\Delta t_r) = \frac{1}{\tau_r^{(j)}} \exp\left[\frac{-\Delta t_r}{\tau_r^{(j)}}\right]. \tag{3.5}$$

A similar process has been considered in a previous paper concerning the clustering of Barkhausen pulses in the magnetization noise.[35] As shown there, $Q(x)$ can be written as

$$Q(x) = Q_1(x) + Q_2(x), \tag{3.6}$$

where

$$Q_1(x) = c_1 \exp(-\mu_1 x), \tag{3.7}$$

$$Q_2(x) = c_2 \exp(-\mu_2 x). \tag{3.8}$$

The quantities c_1, c_2, μ_1, μ_2 appearing in these equations can be related to other three quantities having a clearer physical meaning:

$$\tau_0 = \frac{\int_0^\infty x Q_1(x) dx}{\int_0^\infty Q_1(x) dx}, \tag{3.9}$$

which represents the average time interval between subsequent pulses within the cluster,

$$\rho = \frac{\int_0^\infty Q_1(x) dx}{\int_0^\infty Q_2(x) dx}, \tag{3.10}$$

which represents the average number of pulses within the cluster,

$$\nu_0 = \frac{1}{\langle x \rangle} = \frac{1}{\int_0^\infty x Q(x) dx}, \tag{3.11}$$

which is the average number of pulses per unit time. A further condition is provided by normalization

$$\int_0^\infty Q(x) dx = 1. \tag{3.12}$$

Equations (3.9)–(3.12) allow us to determine the four parameters c_1, c_2, μ_1, μ_2 appearing in $Q(x)$ in terms of τ_0, ρ, ν_0, which can be directly bound to quantities related to the conduction process, as shown in the following. One obtains

$$\tau_0 = \frac{1}{\mu_1}, \quad \rho = \frac{c_1 \mu_2}{c_2 \mu_1}, \quad \nu_0 = \frac{\mu_1^2 \mu_2^2}{(c_1 \mu_2^2 + c_2 \mu_1^2)},$$
$$\frac{c_1}{\mu_1} + \frac{c_2}{\mu_2} = 1. \tag{3.13}$$

The quantities τ_0, ρ, ν_0 characterize a train of pulses of the type described above with

$$\tau_d^{(j)} = \tau_0^{(j)} \rho^{(j)}, \quad \tau_r^{(j)} = \rho^{(j)} \frac{1 - \nu_0^{(j)} \tau_0^{(j)}}{\nu_0^{(j)}}, \tag{3.14}$$

where the index j refers to a particular type of center.

The power spectrum of a pulse train of this type can be calculated by means of a general expression[36]

$$\Phi(\omega) = \nu_0 \Bigg\{ \langle a^2 \rangle \langle |S(\omega)|^2 \rangle + 2\langle a \rangle^2 |\langle S(\omega) \rangle|^2 \times \mathrm{Re}\left[\frac{\int_0^\infty Q(x) e^{i\omega x} dx}{\left[1 - \int_0^\infty Q(x) e^{i\omega x} dx\right]}\right]\Bigg\}, \tag{3.15}$$

where $S(\omega)$ is the Fourier transform of a single pulse of unitary height, a is the pulse height, ν_0 represents the number of pulses per unit time, Re indicates the real part of the expression within square brackets, and $\langle\ \rangle$ indicates an averaging operation over the pulse ensemble. Taking into account Eqs. (3.13), the following expression of the power spectrum is obtained:

$$\Phi(\omega) = \nu_0 \Bigg[\langle a^2 \rangle \langle |S(\omega)|^2 \rangle + 2\langle a \rangle^2 |\langle S(\omega) \rangle|^2 \times \frac{\rho(1 - \nu_0 \tau_0)^2}{\omega^2 \tau_0^2 (\rho + 1 - \rho \nu_0 \tau_0)^2 + 1} \Bigg]. \tag{3.16}$$

It may be pointed out that $\nu_0 \langle a^2 \rangle \langle |S(\omega)|^2 \rangle$ represents the power spectrum of the same pulse sequence in the absence of clustering. The second term within square brackets is thus due to the effect of clustering and, as it will be shown in the following, it is strictly related to the photoinduced noise, i.e., to the noise component arising from the stochastic processes of ionization of photosensitive donor centers, which influence the barrier height. In Eq. (3.16), it is thus possible to distinguish an intrinsic and a photoinduced noise component.

In the following we will apply the general results given by Eq. (3.16) to the case of photoconductors. It is convenient to calculate the conductance fluctuation power spectrum $\Phi_G(\omega)$, since it is independent of the applied voltage. The linearity between applied voltage and photocurrent, for a given light intensity, has been verified for all measurements reported in paper II. Furthermore, the proportionality of the current noise power spectrum to the square of the bias current ensures that noise arises from conductance fluctuations. Conductance pulses are thus proportional to the current pulses introduced above.

According to the model described in Sec. II, each electron injected in the conduction band gives rise to a series of conductance rectangular pulses of height g and duration $\tau_g^{(i)}$. The quantity g is related to the mobility μ of the free electrons by the relationship

$$g=\frac{e\mu}{d^2}\ , \tag{3.17}$$

where d is the distance between the metal electrodes of the device, and e is the elementary charge.

In the present model, the effect of mobility fluctuations will be disregarded, so that in Eq. (3.16) it can be assumed that $\langle a^2\rangle=\langle a\rangle^2=g^2$. In the following, we will refer to a single pulse train of pulses relative to a center j. The total power spectrum will be then obtained by summing up the spectra obtained for each center j. Let $n_g^{(j)}$ be the excess average number of electrons crossing the device during $\tau_d^{(j)}$. According to the model, while $\tau_d^{(j)}$ depends on the particular type of center considered, the average increment of conductance Δg is independent of j and can be written as

$$\Delta g=\frac{n_g^{(j)}}{\tau_d^{(j)}}\frac{e}{V}\ . \tag{3.18}$$

Then the average number of conductance pulses in a cluster is given by

$$\rho^{(j)}=n_g^{(j)}\frac{d^2}{V\mu\tau_g}=\frac{\Delta g}{g}\frac{\tau_d^{(j)}}{\tau_g}\ . \tag{3.19}$$

Equation (3.19) has been obtained from the relationship

$$\rho^{(j)}g\tau_g=\Delta g\,\tau_d^{(j)}\ , \tag{3.20}$$

taking into account Eqs. (3.17) and (3.18).

Another term appearing in the general expression of the spectrum [Eq. (3.16)] is $\nu_0\tau_0$, which can also be expressed in terms of physical quantities characteristic of the photoconductor. Actually, by definition

$$\tau_0^{(j)}=\frac{\tau_d^{(j)}}{\rho^{(j)}}\ , \tag{3.21}$$

$$\nu_0^{(j)}=\frac{\rho^{(j)}}{\tau_d^{(j)}+\tau_r^{(j)}}=\frac{\Delta g}{g}\frac{n^{(j)}}{N^{(j)}}\frac{1}{\tau_g}\ , \tag{3.22}$$

$$\nu_0^{(j)}\tau_0^{(j)}=\frac{\tau_d^{(j)}}{\tau_d^{(j)}+\tau_r^{(j)}}=\frac{n^{(j)}}{N^{(j)}}\ . \tag{3.23}$$

In these equations $n^{(j)}$ is the average number of ionized donor centers of type j in stationary conditions, while $N^{(j)}$ is the total number of these centers. The relation involving these quantities can be written

$$n^{(j)}=\eta^{(j)}n_f\tau_d^{(j)}\frac{N^{(j)}}{N}\ , \tag{3.24}$$

where n_f is the number of photons impinging on the active area of the photoconductor per unit time, $\eta^{(j)}$ is an efficiency factor that depends on λ and may depend on j, and $N^{(j)}/N$ represents the relative number of j centers.

It is useful to introduce an average efficiency factor η_λ depending only on λ,

$$\eta_\lambda=\frac{\sum_j N^{(j)}\eta^{(j)}}{N}\ . \tag{3.25}$$

Then

$$n_d=\sum_j n^{(j)}=\eta_\lambda n_f\sum_j b^{(j)}\tau_d^{(j)}=\eta_\lambda n_f\tau_d\ . \tag{3.26}$$

In this equation

$$b^{(j)}=N^{(j)}\eta^{(j)}\Big/\sum_j N^{(j)}\eta^{(j)} \tag{3.27}$$

represents the ratio of the number of ionizations of the j centers to the total ionization processes, τ_d represents an average time constant weighted over the different j centers, and n_d is the total average number of deep ionized centers.

Substituting into Eq. (3.16) the quantities given by Eqs. (3.19)–(3.23) and multiplying by $N^{(j)}$, the power spectrum of the noise generated by each center j is obtained:

$$\Phi_G^{(j)}(\omega)=N^{(j)}\nu_0^{(j)}g^2\left\{\langle|S(\omega)|^2\rangle+2|\langle S(\omega)\rangle|^2\frac{\dfrac{\Delta g}{g}\dfrac{\tau_d^{(j)}}{\tau_g}\left[1-\dfrac{n^{(j)}}{N^{(j)}}\right]^2}{1+\omega^2\tau_d^{(j)2}\left[1-\dfrac{n^{(j)}}{N^{(j)}}+\dfrac{g}{\Delta g}\dfrac{\tau_g}{\tau_d^{(j)}}\right]^2}\right\}\ . \tag{3.28}$$

The quantity $N^{(j)}\nu_0^{(j)}$ can be obtained from Eq. (3.22) and the final expression of $\Phi_G^{(j)}(\omega)$ becomes

$$\Phi_G^{(j)}(\omega)=gn^{(j)}\Delta g\tau_g\frac{\langle|S(\omega)|^2\rangle}{\tau_g^2}+2n^{(j)}(\Delta g)^2\frac{|\langle S(\omega)\rangle|^2}{\tau_g^2}\frac{\tau_d^{(j)}\left[1-\dfrac{n^{(j)}}{N^{(j)}}\right]^2}{1+\omega^2\tau_d^{(j)2}\left[1-\dfrac{n^{(j)}}{N^{(j)}}+\dfrac{g}{\Delta g}\dfrac{\tau_g}{\tau_d^{(j)}}\right]^2}\ . \tag{3.29}$$

In general, except for very high illumination values, it is reasonable to assume

$$\frac{n^{(j)}}{N^{(j)}} \ll 1 \ . \tag{3.30}$$

It can also be assumed that the quantity

$$\frac{g}{\Delta g}\frac{\tau_g}{\tau_d^{(j)}} \ , \tag{3.31}$$

which, according to Eq. (3.19), represents the inverse of $\rho^{(j)}$, is $\ll 1$. For instance, the data reported in paper II show that this quantity varies from about 10^{-3} at the highest light intensities to about 10^{-1} at the lowest. In this case Eq. (3.29) can be simplified and becomes

$$\Phi_G^{(j)}(\omega)=gn^{(j)}\Delta g\tau_g\frac{\langle |S(\omega)|^2\rangle}{\tau_g^2} +2n^{(j)}(\Delta g)^2\frac{|\langle S(\omega)\rangle|^2}{\tau_g^2}\frac{\tau_d^{(j)}}{1+\omega^2\tau_d^{(j)2}} \ . \tag{3.32}$$

The final step to obtain the whole photocurrent noise power spectrum is to sum over j:

$$\Phi_G(\omega)=\sum_j \Phi_G^{(j)}(\omega) \ , \tag{3.33}$$

which can be written as

$$\Phi_G(\omega)=g\Delta g\tau_g\frac{\langle |S(\omega)|^2\rangle}{\tau_g^2}n_d +2(\Delta g)^2\frac{|\langle S(\omega)\rangle|^2}{\tau_g^2}n_d\sum_j\frac{a^{(j)}\tau_d^{(j)}}{1+\omega^2\tau_d^{(j)2}} \ . \tag{3.34}$$

In Eq. (3.34) $n_d=\sum_j n^{(j)}$ represents the total number of ionized donor centers or trapped holes given by Eq. (3.26) and

$$a^{(j)}=\frac{n^{(j)}}{\sum_j n^{(j)}} \tag{3.35}$$

represents the relative weight of the centers j, having a lifetime $\tau_d^{(j)}$, in determining the actual photoconductance decay after a small pulse of light superimposed on the background illumination. As shown in paper II, the $a^{(j)}$'s and the $\tau_d^{(j)}$'s can be determined from photoresponsivity versus frequency measurements. Also the quantities n_d and Δg will be experimentally determined from measurements of the photoconductance G and of the average relaxation time τ_d versus the photon flux n_f. In particular, τ_d will be obtained as the area to height ratio of the photoconductance relaxation pulse, at different values of the average conductance G and of the light wavelength λ.

The quantities $\langle |S(\omega)|^2\rangle/\tau_g^2$ and $|\langle S(\omega)\rangle|^2/\tau_g^2$, which, according to the model, are independent of the particular center j and depend only on the distribution of the duration of the conductance pulses, can be calculated by means of the distributions given by Eqs. (3.1) and (3.2). Explicit calculations are given in Appendix A.

One obtains

$$\langle |S(\omega)|^2\rangle=\frac{1}{\pi}\left\{\frac{K_1}{\omega}(\arctan\omega\tau_{g2}-\arctan\omega\tau_{g1})+\left[1+K_1\frac{\tau_{g1}-\tau_{g2}}{\tau_{g1}\tau_{g2}}\right]\frac{\tau_s^2}{1+\omega^2\tau_s^2}\right\} , \tag{3.36}$$

$$|\langle S(\omega)\rangle|^2=\frac{1}{2\pi}\left[K_1(\arctan\omega\tau_{g2}-\arctan\omega\tau_{g1})+\left[1+K_1\frac{\tau_{g1}-\tau_{g2}}{\tau_{g1}\tau_{g2}}\right]\frac{\omega\tau_s^2}{1+\omega^2\tau_s^2}\right]^2 + \left[K_1\ln\frac{\tau_{g2}\sqrt{1+\omega^2\tau_1^2}}{\tau_{g1}\sqrt{1+\omega^2\tau_{g2}^2}}+\left[1+K_1\frac{\tau_{g1}-\tau_{g2}}{\tau_{g1}\tau_{g2}}\right]\frac{\tau_s}{1+\omega^2\tau_s^2}\right]^2 , \tag{3.37}$$

$$\tau_g=K_1\ln\frac{\tau_{g2}}{\tau_{g1}}+\left[1+K_1\frac{\tau_{g1}-\tau_{g2}}{\tau_{g1}\tau_{g2}}\right]\tau_s \ . \tag{3.38}$$

The constant K_1 can be expressed in terms of the angular frequency ω_c where the $1/f$ spectrum of the intrinsic noise component crosses the generation-recombination Lorentzian spectrum:

$$K_1=\frac{\omega_c\tau_s^2\tau_{g1}\tau_{g2}}{(\arctan\omega_c\tau_{g2}-\arctan\omega_c\tau_{g1})\tau_{g1}\tau_{g2}(1+\omega_c^2\tau_s^2)+\omega_c(\tau_{g1}-\tau_{g2})\tau_s^2} \ . \tag{3.39}$$

Since at low light intensity the photoinduced noise component becomes negligible, ω_c can be obtained with sufficient accuracy from the experimental spectra.

As shown in Sec. IV, where a detailed discussion of the above results is given, the constants τ_{g1} and τ_{g2} have a negligible influence on all the quantities defined above as long as $\omega\tau_{g1} \ll 1 \ll \omega\tau_{g2}$. This condition is usually assumed to be true in a rather wide range of frequencies.

For what concerns the dependence of Eqs. (3.36) and (3.37) on ω, it can be observed that, under the same condition, $\langle |S(\omega)|^2\rangle/\tau_g^2$ has the expected $1/f$ behavior at low frequencies and tends to become a constant equal to $1/\pi$ at higher frequencies. The constants K_1 and K_2 in Eq. (3.2) determine the relative amplitude of the

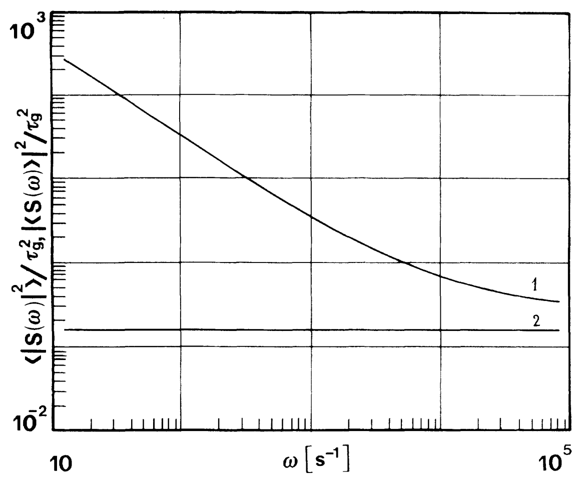

FIG. 1. Behavior of $\langle |S(\omega)|^2\rangle/\tau_g^2$ (curve 1) and $|\langle S(\omega)\rangle|^2/\tau_g^2$ (curve 2) versus frequency. The second of these quantities is a constant equal to $1/2\pi$ and is completely independent of the parameters characterizing the distribution function $P_2(\langle \tau_g^{(j)}\rangle)$ given by Eq. (3.2) if $\omega\tau_{g1} \ll 1 \ll \omega\tau_{g2}$. On the contrary, the first one tends to a constant equal to $1/\pi$ at high frequencies and has a $1/f$ behavior in the low-frequency range. Its actual shape depends on the value of the quantity ω_c.

generation-recombination and flicker noise components characterizing the intrinsic noise. As we will see in paper II, noise measurements at very low light intensity allow us to characterize the distribution given by Eq. (3.2) for the explored frequency range.

The quantity $|\langle S(\omega)\rangle|^2$ is instead a constant equal to $1/2\pi$ even in the low frequency range (see Fig. 1). This means that the spectrum of the photoinduced noise component is essentially a superposition of Lorentzians whose cut-off frequencies are determined only by the values of $\tau_d^{(j)}$. It is not much different from the energy spectrum of the relaxation pulse of the photocurrent after a brief light excitation superimposed on the background radiation.

In the following section a discussion of several aspects of the theoretical noise power spectrum is given.

IV. DISCUSSION

In this section we will consider the influence of different physical quantities, such as light intensity and wavelength, on the noise power spectrum. The main interest concerns the shape and the relative weight of the two noise spectral components given by Eq. (3.34), representing the intrinsic and the photoinduced noise. Anticipating the results of the discussion given below, we can say that at medium to high illumination values the photoinduced noise dominates in the low-frequency range of the spectrum up to a few kHz and is mostly responsible for the abrupt change of the power spectrum amplitude and slope in correspondence to wavelengths near λ_{gap} (see paper II).

We will now discuss separately the behavior of these two components.

Figure 1 shows the behavior of the two dimensionless quantities $\langle |S(\omega)|^2\rangle/\tau_g^2$ and $|\langle S(\omega)\rangle|^2/\tau_g^2$, which, in spite of their rather complicated expressions given by Eqs. (3.36) and (3.37), are only slightly dependent on the actual values of the parameters characterizing the distribution function $P_2(\langle \tau_g^{(i)}\rangle)$, given by Eq. (3.2).

The frequency behavior of the intrinsic component is reported in Fig. 1 (curve 1). Since the photoinduced component becomes smaller than the intrinsic one at low illumination levels, particularly at high frequencies, the value of ω_c appearing in Eq. (3.39) can be determined experimentally. As shown in paper II, for CdS, ω_c depends on λ when λ is near λ_{gap}. This fact can be explained observing that, for $\lambda < \lambda_{\text{gap}}$, light absorption becomes very strong and electrical conduction takes place mostly at the surface. This results in an increment of the $1/f$ noise component.

Another important aspect of the intrinsic spectral component lies in the behavior of its amplitude versus light intensity. Since the quantity $\Delta g n_d$, from the data reported in paper II, turns out to be nearly proportional to G, this amplitude is expected to drop as $1/G$, a fact that is well supported experimentally in a range of G values covering about three orders of magnitude.

Since $|\langle S(\omega)\rangle|^2/\tau_g^2$ is practically a constant close to $1/2\pi$, the shape of the photoinduced spectral component is determined by the quantity

$$\sum_j \frac{a^{(j)}\tau_d^{(j)}}{1+\omega^2\tau_d^{(j)2}} , \tag{4.1}$$

which is a weighted superposition of Lorentzian spectra.

The abrupt change of the noise power spectrum observed in different photoconductors (CdS and CdSe) when λ equals λ_{gap} can thus be explained taking into account that the $\tau_d^{(j)}$'s distribution depends strongly on the light wavelength λ in the vicinity of λ_{gap}. Let us assume, for simplicity, that a single lifetime τ_d dominates the spectrum of the $\tau_d^{(j)}$'s. Then, at frequency values where $\omega^2\tau_d^2 \gg 1$, but the photoinduced component is still much larger than the intrinsic one, the relative change of the power spectral density is given by the ratio

$$\frac{\tau_d(\lambda > \lambda_{\text{gap}})}{\tau_d(\lambda < \lambda_{\text{gap}})} . \tag{4.2}$$

For CdS this ratio turns out to be about 10 (see Fig. 13 of paper II) and is actually in good agreement with the ratio of the power spectral densities measured at two wavelengths λ above and below λ_{gap} in the range of frequencies between 10 Hz and 1 kHz, as shown in Figs. 4 and 5 of paper II.

At high-frequency values (typically above 10 kHz for CdS) the change of the photoinduced noise component does not influence the total noise power density, since, owing to its $1/f^2$ slope, it drops below the intrinsic component. Thus at high frequency the noise power density becomes insensitive to λ, as confirmed by experiments.

A final point to be discussed is the behavior of the amplitude of the photoinduced component when the light intensity is changed. Since the intrinsic component amplitude of $\Phi_G(\omega)/G^2$ behaves as $1/G$, it is sufficient to consider the behavior of the ratio between the amplitudes of the photoinduced and of the intrinsic component versus electrical conductance G. Considering only the quantities that depend on G, this ratio is proportional to the quantity

$$\frac{\Delta g}{g}\sum_j \frac{a^{(j)}\langle \tau_d^{(j)}\rangle}{1+\omega^2\langle \tau_d^{(j)}\rangle^2} . \tag{4.3}$$

According to the fact that $\Delta g/g$ increases with the light intensity approaching 1 at the highest values, it is expected that the amplitude of the photoinduced component drops with a slope smaller than $1/G$. This prediction is also confirmed by experiments, as shown in paper II.

V. SUMMARY

A theory of current noise in CdS photoconducting devices based on a barrier-type photoconduction model is presented. The transport process is described as a stream of conduction electrons crossing a potential barrier, whose height depends on the positive trapped charge produced by light (trapped holes or ionized deep donor centers) and has a normal fluctuation related to the fluctuation of this charge. A general formula of the power spectrum of pulse trains, characterized by a set of probability density functions describing their slope, amplitude, and time distributions has been used to work out the photoconductance noise power spectrum of the device. The final expression consists of two components which are related to different aspects of the fluctuation process. One component corresponds to an intrinsic noise produced by the transport process within the photoconducting material and consists of the generation-recombination and flicker noise contributions, while the other one is generated by the fluctuation of the potential barrier height (photoinduced noise component). All quantities appearing in this expression have a clear physical meaning and can be measured by suitable experiments on the photoconducting device. Thanks to this, a thorough check of the noise theory and of the barrier photoconduction model on which the theory is based is reported in paper II and in Appendix B.

ACKNOWLEDGMENT

The authors wish to thank Professor C. M. Van Vliet for reading the manuscript and making useful suggestions.

APPENDIX A

In this appendix, the evaluation of $\langle |S(\omega)|^2\rangle$ and $|\langle S(\omega)\rangle|^2$ will be performed using the probability density function introduced in Sec. III,

$$P_2(\langle \tau_g^{(i)}\rangle)=K_1\frac{1}{\langle \tau_g^{(i)}\rangle^2}+K_2\delta(\langle \tau_g^{(i)}\rangle-\tau_s) . \tag{A1}$$

The normalization condition

$$\int_0^\infty P_2(\langle \tau_g^{(i)}\rangle)d\langle \tau_g^{(i)}\rangle=1 \tag{A2}$$

gives

$$K_2=1+K_1\left[\frac{\tau_{g1}-\tau_{g2}}{\tau_{g2}\tau_{g1}}\right] . \tag{A3}$$

The Fourier transform of an elementary rectangular pulse of length $\langle \tau_g^{(i)}\rangle$ is given by

$$S(\omega,\langle \tau_g^{(i)}\rangle)=\frac{1}{\pi}\frac{i\langle \tau_g^{(i)}\rangle}{1+i\omega\langle \tau_g^{(i)}\rangle} . \tag{A4}$$

The mean value of the square modulus of this quantity becomes

$$\begin{aligned}\langle |S(\omega,\langle \tau_g^{(i)}\rangle)|^2\rangle &=\int_0^\infty |S(\omega,\langle \tau_g^{(i)}\rangle)|^2 P_2(\langle \tau_g^{(i)}\rangle)d(\langle \tau_g^{(i)}\rangle)\\ &=\frac{1}{\pi}\left[\frac{K_1}{\omega}(\arctan\omega\tau_{g2}-\arctan\omega\tau_{g1})+K_2\frac{\tau_s^2}{1+\omega^2\tau_s^2}\right] ,\end{aligned} \tag{A5}$$

while the square modulus of its mean value is

$$\begin{aligned}|\langle S(\omega,\langle \tau_g^{(i)}\rangle)\rangle|^2 &=\left|\int_0^\infty S(\omega,\langle \tau_g^{(i)}\rangle)P_2(\langle \tau_g^{(i)}\rangle)d(\langle \tau_g^{(i)}\rangle)\right|^2\\ &=\frac{1}{2\pi}\left|\left\{K_1(\arctan\omega\tau_{g2}-\arctan\omega\tau_{g1})+K_2\frac{\omega\tau_s^2}{1+\omega^2\tau_s^2}\right\}-i\left\{K_1\ln\frac{\tau_{g2}\sqrt{1+\omega^2\tau_{g1}^2}}{\tau_{g1}\sqrt{1+\omega^2\tau_{g2}^2}}+K_2\frac{\tau_s}{1+\omega^2\tau_s^2}\right\}\right|^2\\ &=\frac{1}{2\pi}\left\{K_1(\arctan\omega\tau_{g2}-\arctan\omega\tau_{g1})+K_2\frac{\omega\tau_s^2}{1+\omega^2\tau_s^2}\right\}^2+\left\{K_1\ln\frac{\tau_{g2}}{\tau_{g1}}\frac{\sqrt{1+\omega^2\tau_{g1}^2}}{\sqrt{1+\omega^2\tau_{g2}^2}}+K_2\frac{\tau_s}{1+\omega^2\tau_s^2}\right\}^2 .\end{aligned} \tag{A6}$$

The parameter K_1 appearing in these equations can be expressed in terms of the quantity ω_c, defined in Sec. III as the angular frequency where the $1/f$ and the Lorentzian spectral component intersect:

$$\frac{K_1}{\omega_c}(\arctan\omega_c\tau_{g2}-\arctan\omega_c\tau_{g1})=\left[1+K_1\frac{\tau_{g1}-\tau_{g2}}{\tau_{g1}\tau_{g2}}\right]\frac{\tau_s^2}{1+\omega_c^2\tau_s^2}\ . \tag{A7}$$

One gets

$$K_1=\frac{\omega_c\tau_s^2\tau_{g1}\tau_{g2}}{(\arctan\omega_c\tau_{g2}-\arctan\omega_c\tau_{g1})\tau_{g1}\tau_{g2}(1+\omega_c^2\tau_s^2)+\omega_c(\tau_{g1}-\tau_{g2})\tau_s^2}\ . \tag{A8}$$

$$\tau_g=\int_{\tau_{g1}}^{\tau_{g2}}\langle\tau_g^{(i)}\rangle P_2(\langle\tau_g^{(i)}\rangle)d\langle\tau_g^{(i)}\rangle=K_1\ln\frac{\tau_{g2}}{\tau_{g1}}+K_2\tau_s\ . \tag{A9}$$

Using Eqs. (A3) and (A8), Eqs. (A5) and (A6) can be expressed in terms of ω_c, and Eqs. (3.36)–(3.38) are obtained.

APPENDIX B

In this appendix it will be shown that the barrier photoconduction model, used to develop the photocurrent noise theory, permits us to obtain a good fit of the curves of the photoconductance versus light intensity reported in paper II. Even if this calculation is not necessary to the development of the photoconductance noise theory, it is given here since it shows that the same parameters reproducing the noise power spectrum in different light conditions also give the right photoconductance value. It should be pointed out, however, that several further assumptions made here, such as, for instance, the specific transport mechanism through the potential barrier, are not needed to calculate the noise power spectrum. In fact, whatever the dependence of photoconductance G on the number of ionized centers n_d, linearization is always possible for the small fluctuations causing the noise.

As already stated, we consider a CdS-based photoconducting device with indium electrodes making ohmic contacts.[26] It is further assumed that the Fermi level of CdS is far from the conduction band, as appropriate to a nearly intrinsic material or to a material characterized by deep donor centers. In the absence of surface states, taking into account the values of the indium work function $\phi_m=4.12$ eV (Ref. 37) and of the CdS electron affinity $\chi_s=4.79$ eV,[38] in thermal equilibrium the energy band scheme in correspondence of the metal-electrode interface is represented in Fig. 2. Indium diffusion within CdS would change this situation a little by anchoring the Fermi level slightly below the conduction band at the CdS surface. In any case, an accumulation layer is formed in correspondence to the metal-photoconductor interface, which does not work as a *virtual cathode,* since a barrier (whose height $\phi_s-\chi_s$ is of the order of 1 eV for near-intrinsic CdS) is created by the band bending near the interface.[39] It is well known that in this situation in the presence of light, a nonequilibrium stationary condition is reached where the potential barrier is lowered by a trapped positive charge.[40] To evaluate the dependence of the barrier height on the light intensity, we will consider the effect of the space charge, under steady light conditions, on the band structure represented in Fig. 2. The space charge consists of a positive static charge uniformly distributed in the photoconducting film due to ionized deep donor centers or to trapped holes, according to the light wavelength, and of a negative mobile charge constituted by electrons injected from the cathode into the conduction band of the photoconducting material.

As shown in the following, at high illumination values the barrier height is controlled by the feedback effect of the negative injected charge and a linear behavior of the device photoconductance versus light intensity is reached. At low light intensity, since the feedback effect becomes negligible, an exponential-like behavior of the photoconductance versus light intensity is expected.

In a single barrier mechanism of charge transport, considering a thermally activated process, the conductivity is given by[23]

$$\sigma=\frac{2}{h^3}(2\pi m^*kT)^{3/2}\exp\left[-\frac{\phi_M}{kT}\right]e\mu\ , \tag{B1}$$

where m^* is the effective mass of the electrons, k is the Boltzmann constant, h is the Planck constant, T is the absolute temperature, e is the elementary charge, μ is the electron mobility, and ϕ_M is the barrier height. As already mentioned, in the dark the barrier height ϕ_M is given by the difference between the extraction potential ϕ_s and the electron affinity χ_s,

$$\phi_M=\phi_s-\chi_s=\phi_0\ , \tag{B2}$$

According to Eq. (B1), this barrier reduces the conductivity, as expected for a metal-insulator contact. The

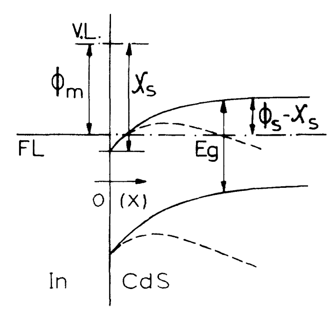

FIG. 2. Ideal energy-band diagram at the interface In-CdS. According to Refs. 37 and 38, $\phi_m=4.12$ eV, $\chi_s=4.79$ eV, and $E_{\text{gap}}=2.49$ eV. The barrier $\phi_s-\chi_s$ depends on doping. To fit the data reported in Fig. 3, a dark barrier height of 0.54 eV is needed. The band bending and the corresponding lowering of the barrier in the presence of light (dotted lines) is given by Eqs. (B4) and (B5). The contact may be defined as ohmic since the condition $\phi_m\le\chi_s$ holds, but it does not work as a *virtual cathode* in the dark owing to the presence of the barrier.

function describing the barrier shape along the x direction (see Fig. 2) can be written, as a good approximation, in the following form:

$$\phi(x)=\phi_0(1-e^{x/L_D}) , \quad \text{(B3)}$$

where L_D is the effective Debye length.[41] In the presence of light a positive trapped charge is created and the barrier height is lowered, giving rise to the photoconduction process.

Let n_d^* be the density of ionized donor centers or trapped holes and n_e^* the density of the electrons thermally injected from the cathode into the conduction band of the photoconductor. The electric field created by this charge, uniformly distributed within the photoconducting film, is proportional to the net charge and may be considered constant for distances of the order of L_D, since $L_D \ll d$, near the metal electrodes. This corresponds to approximating the parabolic potential created by the charge with its tangent near the metal electrode. Then

$$\phi(x)=\phi_0\left[1-\exp\left[\frac{x}{L_D}\right]\right]-eE_0(n_d^*-n_e^*)x , \quad \text{(B4)}$$

where E_0 is an appropriate constant whose value will be discussed in the following. The maximum value ϕ_M of $\phi(x)$ can be found from Eq. (B4) by putting $d\phi(x)/dx=0$:

$$\phi_M=\phi_0-L_DeE_0(n_d^*-n_e^*)\left[1+\ln\frac{\phi_0}{L_DeE_0(n_d^*-n_e^*)}\right] . \quad \text{(B5)}$$

The quantity n_e^* is related to the photoconductance G of the devices through the equation

$$G=n_e^*\frac{e\mu S}{d} , \quad \text{(B6)}$$

where S is the photoconducting film cross-section area and d the distance between electrodes. From Eqs. (B1), (B5), and (B6) one finally gets

$$G=G_0\exp\left\{\frac{L_DeE_0}{kT}\left[n_d^*-\frac{Gd}{e\mu S}\right]\times\left[1+\ln\frac{\phi_0}{L_DeE_0\left[n_d^*-\frac{Gd}{e\mu S}\right]}\right]\right\} , \quad \text{(B7)}$$

where

$$G_0=\frac{2}{h^3}(2\pi m^*kT)^{3/2}\exp\left[-\frac{\phi_0}{kT}\right]e\mu\frac{S}{d} . \quad \text{(B8)}$$

This last quantity represents, to a good approximation, the dark electrical conductance of the device.

Equation (B7) gives an implicit relationship between the photoconductance G and the positive static charge density n_d^* which can be solved by numerical standard methods. It reproduces the experimental behavior of the photoconductance G versus the total number of ionized donor centers or trapped holes n_d, as Fig. 3 shows. The quantity $n_d=n_d^*Sd$ is related to the photon flux n_f by Eq. (3.26). Experimental data are taken from the results reported in Fig. 14 of paper II, which also show that photoconductance becomes closely independent of the light wavelength λ, when expressed in terms of n_d, as expected from the present photoconduction model. Theoretical curves are obtained from Eq. (B7), introducing the cross section $S=1.5\times10^{-6}\times2\times10^{-2}$ m^2 and the interelectrodic distance $d=1$ mm. The dark barrier height ϕ_0 has been derived using Eq. (B8) and the experimental value of the dark conductance G_0 of the device ($G_0=4\times10^{-10}$ S), taking into account that the electron effective mass for CdS is 0.2 times the electron rest mass and the relative dielectric constant is $\epsilon_r\cong9\epsilon_0$.[42]

The factor L_DeE_0, which determines the initial slope of the photoconductance curve in the semilogarithmic plot of Fig. 3, has been obtained as a best-fit parameter for the experimental curve ($L_DeE_0\cong9\times10^{-41}$ J m^3). Even if the exactness of this value cannot be proved directly, since the value of L_D is not known, it can be shown that it is physically senseful. Actually, since the quantity E_0 represents the electric field due to a uniform charge density corresponding to a single ionized donor center or

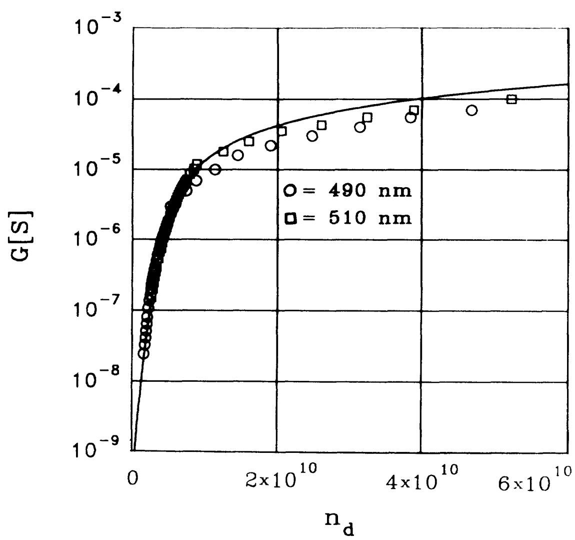

FIG. 3. Comparison between experimental (dots and squares) and theoretical (full line) results concerning the behavior of photoconductance G versus the total number n_d of ionized donor centers ($\lambda>500$ nm) or trapped holes ($\lambda<500$ nm) for the photoconducting device described in Sec. II of this paper. While the behavior of G versus n_f is very different as the wavelength is changed (see Sec. II), the behavior of G versus n_d is very closely independent of λ, in agreement with the barrier model developed here. Fitting is good for the whole range of photoconductance values explored. The parameters are the same used to reproduce the photocurrent noise spectra reported in Sec. II.

trapped hole per unit volume, averaged over a length L_D near the metal electrode, an approximated evaluation of L_D can be worked out.

Numerical calculations of the tangential component of the electric field in correspondence with the metal electrode give the approximate value of $E_0 = 1 \times 10^{-15} n_d^*$ V m^{-1}. This value corresponds to a Debye length $L_D = 0.5$ μm, which does not seem unreasonable.

[1]K. M. Van Vliet and J. Blok, Physica **22**, 231 (1956).

[2]K. M. Van Vliet and J. Blok, Physica **22**, 525 (1956).

[3]K. M. Van Vliet, Phys. Rev. **133**, A1182 (1964).

[4]K. M. Van Vliet, Physica **83B**, 52 (1976).

[5]K. M. Van Vliet, J. Blok, C. Ris, and J. Steketee, Physica **22**, 723 (1956).

[6]R. L. Petritz, Phys. Rev. **104**, 1508 (1956).

[7]F. L. Lummis and R. L. Petritz, Phys. Rev. **105**, 502 (1957).

[8]J. J. Brophy and R. J. Robinson, J. Appl. Phys. **31**, 8 (1960).

[9]J. J. Brophy and R. J. Robinson, Phys. Rev. **117**, 3 (1960).

[10]J. J. Brophy, Phys. Rev. **119**, 2 (1960).

[11]J. J. Brophy, Phys. Rev. **122**, 1 (1961).

[12]J. J. Zijlstra and A. Van der Ziel, Physica **29**, 78 (1963).

[13]J. J. Zijlstra and A. Van der Ziel, Physica **29**, 851 (1963).

[14]S. Kruizinga and J. J. Zijlstra, Phys. Lett. **28A**, 399 (1968).

[15]J. P. Vilcot, M. Constant, D. Decoster, and R. Fauquembergue, Physica B **129**, 488 (1985).

[16]G. J. Papaionnaou, J. Appl. Phys. **72**, 5269 (1992).

[17]J. T. Ubbink, Physica **52**, 253 (1971).

[18]D. L. Smith, J. Appl. Phys. **53**, 7051 (1982).

[19]A. Carbone and P. Mazzetti, in *Noise in Physical Systems and 1/f Fluctuations,* edited by Peter H. Handel and Alma L. Chung (AIP Press, New York, 1993).

[20]A. Carbone, F. Demichelis, and P. Mazzetti, in *Optical Materials: Processing and Science,* edited by D. B. Poker and C. Ortiz, MRS Symposia Proceedings No. 152 (Materials Research Society, Pittsburgh, 1989), p. 163.

[21]R. H. Bube, *Photoconductivity of Solids* (Wiley, New York, 1964).

[22]R. H. Bube, *Photoelectronic Properties of Semiconductors* (Cambridge University Press, Cambridge, England, 1992).

[23]J. C. Slater, Phys. Rev. **103**, 1631 (1956).

[24]A. F. Gibson, Proc. Phys. Soc. **65B**, 196 (1952).

[25]R. M. Westervelt and S. W. Teitsworth, J. Appl. Phys. **57**, 5457 (1985).

[26]R. W. Smith, Phys. Rev. **97**, 1525 (1955).

[27]A. Van der Ziel, *Solid State Physical Electronics* (Prentice Hall, Englewood Cliffs, NJ, 1976).

[28]R. L. Stratonovich, *Topics in the Theory of Random Noise* (Gordon and Breach, New York, 1967), Vol. I.

[29]A. Van der Ziel, *Fluctuation Phenomena in Semi-Conductors* (Butterworth Scientific, London, 1959).

[30]A. L. Mc Worther (unpublished).

[31]D. Halford, Proc. IEEE **56**, 251 (1968).

[32]R. E. Burgess, British J. Appl. Phys. **6**, 185 (1955).

[33]Th. M. Nieuwenhuizen and M. H. Ernst, Phys. Rev. **33**, 2824 (1986).

[34]*Proceedings of the 11th International Conference on Noise in Physical System and 1/f Fluctuations,* edited by T. Musha, S. Sato, and M. Y. Amamoto (Ohmsha Ltd., Kyoto, 1991).

[35]P. Mazzetti A. Ferro, and G. Montalenti, Il Nuovo Cimento **56B**, 111 (1968).

[36]P. B. Mazzetti, Il Nuovo Cimento **31**, 88 (1964).

[37]*CRC Handbook of Chemistry and Physics* (CRC, Boca Raton, FL, 1978).

[38]J. L. Freeouf and J. M. Woodall, Appl. Phys. Lett. **39**, 727 (1981).

[39]A. Rose, Phys. Rev. **97**, 1538 (1955).

[40]A. Many, Y. Goldstein, and N. B. Grover, Semiconductor Surfaces (North-Holland, Amsterdam, 1971).

[41]*Polycrystalline Semiconductors,* edited by H. J. Moller, H. P. Strunk, and J. H. Werner (Springer-Verlag, Berlin, 1989).

[42]*Data in Science and in Technology: Semiconductors,* edited by O. Madelung (Springer-Verlag, Berlin, 1992).

[43]S. Machlup, J. Appl. Phys. **25**, 341 (1954).